

## ARTICLES

## A Study of the Effects of Europium Doping and Calcination on the Luminescence of Titania Phosphor Materials

James Ovenstone,\* Philip. J. Titler, Robert Withnall, and Jack Silver\*

*School of Chemical and Life Sciences, University of Greenwich, Island Site, Woolwich, London SE18 6PF**Received: November 9, 2000; In Final Form: April 8, 2001*

A range of europium-activated titania phosphors with the formula  $\text{Ti}_{1-3x}\text{Eu}_{4x}\text{O}_2$  ( $x$  varying between 0.000397 and 0.00794) have been prepared, and the effects of europium content and titania phase on the luminescent properties have been investigated. It has been demonstrated that the crystallization temperature of the titania from the amorphous phase to the anatase phase is raised by addition of europium to the material. At the same time, the brightness of the emission is also increased as the europium content is raised to  $x = 0.00794$ . In addition, we have shown that calcination of the titania to form anatase or rutile reduces the brightness of the luminescence, and that as the temperature of calcination increases, the brightness falls.  $^{151}\text{Eu}$  Mössbauer spectroscopy results have shown evidence for the presence of multiple sites (by line broadening) as the europium concentration increases. Extra sites were also observed as the firing temperature was increased. In the most extreme cases, the second sites are clearly visible as extra peaks. The Mössbauer spectrum for hydrothermally produced material (which showed no luminescence) was relatively narrow, indicating that only one site was present for the europium in this phase. These results indicate that the multiple sites observed for the europium in the calcined samples result from the europium doping into both the anatase lattice and the brookite contaminant lattice, and it is this latter material that is responsible for the luminescence in the metastable crystalline titania.

## Introduction

Europium 3+ ions are well-known as activator dopants for many different inorganic lattices producing bright red luminescent phosphors.<sup>1</sup> The red color is due to the electric dipole transitions of electrons from the  $^5\text{D}_0$  level to the  $^7\text{F}_2$  level. However, the emission is not entirely controlled by the europium 3+ ions, since the host lattice also plays an important role. If a europium site has no inversion symmetry (as observed in most commercial phosphors) the strong emission is in the range 610 to 630 nm, whereas, if the europium site has inversion symmetry (as in  $\text{Ba}_2\text{GdNbO}_5$ ) then one would expect the emission line to come in the region 580–600 nm.<sup>2</sup> The excitation wavelength is also affected by the lattice; for example, europium-doped yttrium oxide is most efficiently excited by short wavelength UV radiation (254 nm), to give a bright emission at 611 nm, while lanthanum oxide doped with europium emits at 615 nm, and is better excited with long wavelength UV light (366 nm).<sup>3</sup>

Until recently, most research into photoluminescence (PL) phosphors concentrated on materials which could be excited at either 254 or 366 nm to produce bright emissions in the visible part of the electromagnetic spectrum. This was because these wavelengths represent the major emissions from mercury lamps which have been the mainstay for PL excitation for decades. With the advent of new display technologies, and the huge leaps forward in other light-emitting technologies, such as light-emitting diodes (LEDs), there is increasing scope for the

application of phosphors excited in other regions of the electromagnetic spectrum.<sup>4</sup>

Titania is well-known as a powerful photocatalyst, capable of accelerating many different reactions, such as the oxidation of organic acids to  $\text{CO}_2$ , and even the photolysis of water.<sup>5–9</sup> The mechanisms for these reactions are not entirely understood, but it is generally accepted that the process begins with UV light stimulating the production of free electrons and positive holes within the titania lattice. These charged species then either recombine (resulting in no useful chemistry), or move apart. If they can reach the surface of the titania particles, they can interact with surface-adsorbed molecules, forming radical species which then go on to perform the useful chemical reactions.<sup>10</sup>

In view of this strong interaction with UV light, it was decided to investigate the potential of the titania lattice as a potential host lattice for phosphors. Titania has three naturally occurring crystalline polymorphs, which can be formed by calcination of the amorphous material. The first to form is anatase, and then at high temperatures ( $>800\text{ }^\circ\text{C}$ ) the rutile phase. The brookite phase is generally formed as a secondary product together with anatase, but is eliminated as the calcination temperature is increased, leaving only the anatase product. Preliminary work indicated that titania could easily be doped with europium. Doping could be achieved in the amorphous state, and then the powder fired at different temperatures to produce the various polymorphs.

In this initial study, the effect the addition of europium has on the formation of the different structures, and also the usefulness of the various polymorphs as phosphors is reported.

\* Authors to whom correspondence should be addressed.

The latter aim is of particular interest, since the various polymorphs have different band gap energies (3.0 eV for rutile, and 3.2 eV for anatase).<sup>11</sup> This was indicative that not only would their efficiencies as phosphor lattices vary considerably, but also the excitation wavelengths should also vary.

## Experimental Section

### Preparation of Amorphous Europium-Doped Titania.

TiCl<sub>4</sub> (20 mL; Fluka) was dropped into ice cold water (200 mL) with rapid mixing. Some turbidity was observed, but disappeared over time (24 h). Eu(NO<sub>3</sub>)<sub>3</sub> was prepared by dissolving Eu<sub>2</sub>O<sub>3</sub> (Aldrich) in a stoichiometric amount of concentrated nitric acid to form a 0.1 M stock solution. Appropriate quantities of europium nitrate solution were then added to 20 mL of the TiCl<sub>4</sub> solution to give product stoichiometries (Ti<sub>1-3x</sub>Eu<sub>4x</sub>O<sub>2</sub>;  $x$  varying between 0.000397 and 0.00794). The mixtures were then added dropwise into 100 mL of 7.3 M ammonia solution (large excess) with rapid mixing. The precipitate was aged for 20 min before being filtered and washed with water to remove excess base. The powder was then dried in an oven at 65 °C for 24 h.

X-ray powder diffraction (XRD) was carried out using a Philips pw1710 diffractometer. A step size of 0.02° 2 $\theta$  was used with a scan speed of 0.5° per minute. Raman spectra were obtained using a Labram Raman spectrometer equipped with an 1800 g/mm holographic grating, a holographic supernotch filter, and a Peltier-cooled CCD detector. Samples were excited using a helium–neon laser with an output of 8 mW of power at the sample on the 632.8 nm line. XRD and Raman spectroscopy showed that the initial powders were indeed amorphous, and free from any crystalline titania phases. For XRD, no peaks were observed, while the Raman spectra did not exhibit any strong bands at 398, 514, and 641 cm<sup>-1</sup> (anatase) or 448 and 612 cm<sup>-1</sup> (rutile), which would be expected even if nanocrystalline material was present. The Raman spectrometer was used both to obtain Raman spectra of the samples and to observe Stokes luminescence spectra, excited by the 632.8 nm laser line.

**Preparation of Crystalline Titania.** The samples prepared as above were calcined in a furnace at various temperatures from 300 °C to 1000 °C for 1 h. The calcinations were carried out in alumina crucibles in a static air atmosphere. XRD was used to determine the phase of each of the products.

Some of the amorphous powder was also crystallized using the hydrothermal method. In this case, the  $x = 0.00318$  europium sample was used as the starting material. A 0.3 g sample of amorphous powder was suspended in 35 mL of distilled water in a sealed vessel. The vessel was then heated using microwaves (CEM MDS-2100 microwave autoclave system) to 200 °C for 2 h before being allowed to cool. The powder was then filtered and dried in an oven at 65 °C for 24 h. XRD and Raman spectroscopy confirmed that the product was phase pure anatase.

**Measurement of Luminescence Properties.** Photoluminescence brightness measurements were made using a Pritchard PR880 photometer. The powders were packed into a glass holder approximately 0.5 mm deep, and with an area approximately 1.5 cm  $\times$  1 cm. The surface was smoothed using a glass slide, and then illuminated with a 100W UV lamp emitting light at 366 nm.

Emission and excitation spectra were measured using a customized system. Excitation wavelengths were selected from a Xenon Lamp (Bentham, type IL7D), using a Bentham M300BA monochromator. Samples were placed in a Bentham SC–FLUOR fluorescence chamber, and the emission wave-

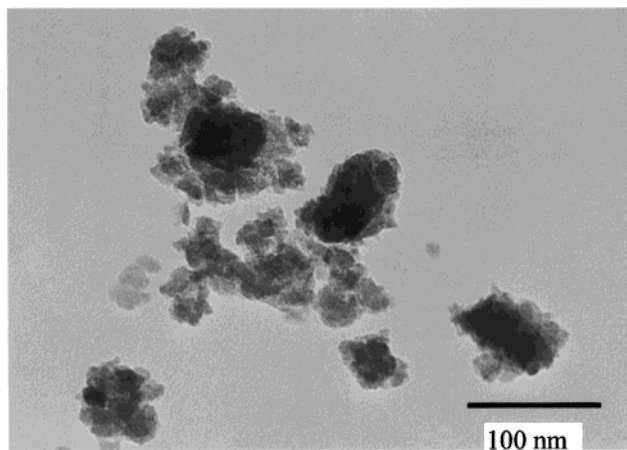


**Figure 1.** TEM micrograph of unfired titania powder containing a europium content of  $x = 0.00318$ .

lengths measured using another M300BA monochromator. The emission spectra were measured for an excitation wavelength of 366 nm.

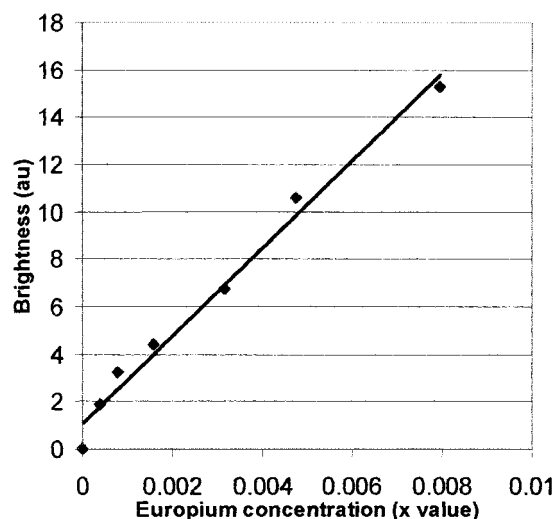
**General Characterization.** Differential scanning calorimetry (DSC; Perkin-Elmer DSC7 machine connected to a TAC7/3 instrument controller) was used to determine the crystallization temperature of the anatase phase in each of the powders produced. The specific surface areas of the powders were determined by the BET method (Micromeritics Gemini 2375). TEM was carried out using a JEOL J200-CX machine. Europium contents were measured by dissolving the samples in hydrochloric acid and then analyzing by ICPMS (Perkin-Elmer Elan 5000).

<sup>151</sup>Eu Mössbauer spectra were recorded using a modification of the previously reported<sup>12</sup> transmission setup. The spectra were recorded at 78 K with a 200 mCi Amersham <sup>151</sup>SmF<sub>3</sub> source attached to the velocity transducer. The experimental line width for the above source is 2.4 mms<sup>-1</sup> (298 K).<sup>13</sup> The transmitted 21.6 keV gamma signal was detected by a Canberra 1662B X-ray scintillation detector. The resulting spectral data sets were collected on a PC via a Wissel CMCA-550 ISA data collection card utilizing Wissoft'98 collection software. The data sets were then fitted to Lorentzian line shapes using Wissel Normos Version 9.0. Spectra are quoted with respect to EuF<sub>3</sub> (298 K). Spectrometer calibration was carried out using a AEA 25 mCi <sup>57</sup>Fe source and 25  $\mu$ m natural iron foil. As the samples contained only small amounts of europium, and the sample weights were constant, change in the observed line widths are regarded as outside experimental error.

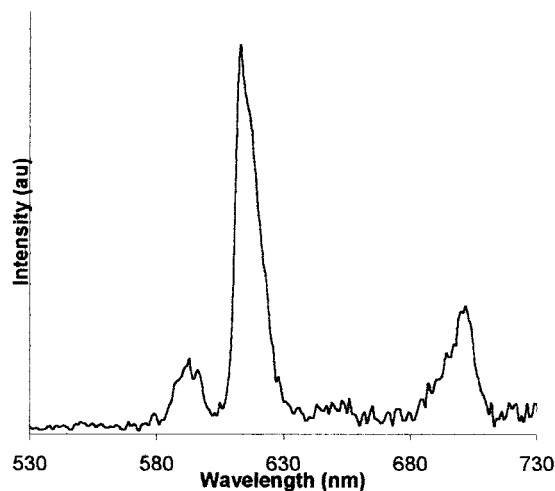
## Results and Discussion

Figure 1 shows a TEM micrograph of the amorphous titania. The primary particles are approximately 10 nm or less in size, and loosely clustered into agglomerates up to around 100 nm. BET measurements indicated the surface area of the powder was high (around 150 m<sup>2</sup>g<sup>-1</sup>). The microstructure and surface area exhibited no noticeable changes when up to a Eu<sup>3+</sup> concentration of  $x = 0.00794$  was introduced into the material.

**Effect of Changing the Europium Doping Concentration.** Brightness measurements were obtained for unfired powders with different europium concentrations. The brightness was observed to increase linearly with europium content from  $x = 0.000397$  to  $x = 0.00794$  (Figure 2). Although the brightness of the material cannot compete with a commercial phosphor (the measured PL value for YVO<sub>4</sub>:Eu from Phosphor Technology is approximately 12 times brighter than the  $x = 0.00397$



**Figure 2.** Graph of emission photoluminescence brightness vs europium content for unfired samples. Samples are excited using a 366 nm lamp and brightness measured using a photometer.



**Figure 3.** Typical emission spectrum for europium-doped titania (unfired). This sample contained a europium content of  $x = 0.00794$ .

material produced here), this material is the first reported amorphous inorganic rare earth doped powder phosphor. In addition, the concentration of activator producing the brightest emission has not yet been attained. Figure 3 shows a typical emission spectrum for europium doped titania. There is a main emission peak at 614 nm, and also, at higher concentrations, two satellite peaks at 592 and 702 nm develop. The laser Raman spectrometer was used to observe the latter emission peak as it developed. From Figure 4, it can be seen that at a europium concentration of  $x = 0.000397$ , there is almost no emission at 702 nm. Even at this low concentration, however, the material clearly emits red light under UV (the peak at 614 nm), and so this may point to the emissions at 614 and 702 nm coming from different sources.

To investigate this possibility further, europium Mössbauer spectroscopy was employed to determine if any large changes in the europium environment could be detected as the europium concentration was increased. The spectra for the powders exhibited increasingly broad peaks (Figure 5) with increasing europium concentration, indicating the development of multiple europium environments within the amorphous material. The isomer shifts show small changes first to smaller isomer shift then to larger. We believe that as only the higher concentrations of  $\text{Eu}^{3+}$  cause larger isomer shifts, this suggests more environ-

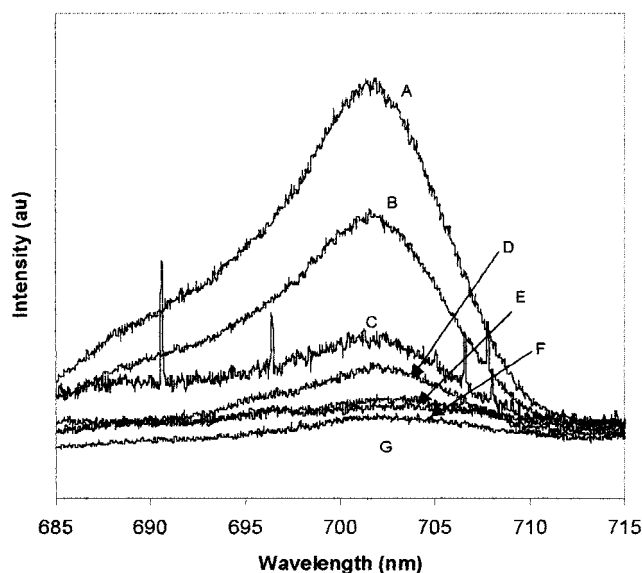


**Figure 4.** Down conversion luminescent spectra obtained, using a Raman spectrometer, of europium emission bands for unfired samples with various europium concentrations. (A)  $x = 0.00794$ , (B)  $x = 0.00476$ , (C)  $x = 0.00318$ , (D)  $x = 0.00159$ , (E)  $x = 0.000794$ , (F)  $x = 0.000397$ , and (G) hydrothermal ( $x = 0.00318$ ).

ments are present as the spectra were only fitted for single peaks and hence the "total" isomer shift has little meaning. Table 1 presents the data for the peak widths and the isomer shifts for the different materials.

Excitation spectra for the samples' different emissions were also measured. Figure 6 presents the excitation spectra for the sample doped with a europium concentration at  $x = 0.00794$ . The spectra show the wavelengths of excitation energy which cause the emissions at 592, 614, and 702 nm. The spectra have been normalized around the peak at 400 nm. From these data, it is quite clear that  $\text{Ti}_{1-3x}\text{Eu}_x\text{O}_2$  should not be excited by 254 nm radiation, and that even 366 nm radiation will be a poor choice. Instead, the most efficient excitation wavelengths are at longer wavelengths, i.e., 397, 466, and 536 nm. In addition, it can also be seen that the different emission peaks are not equally excited by the different excitations. Both the emission peak at 592 nm and the peak at 702 nm are excited most efficiently by 397 nm radiation, and considerably less by the longer wavelength excitations. The main emission peak at 614 nm, however, is almost equally well excited by all three excitation wavelengths. Therefore, by careful choice of the excitation wavelength, the color of emission can be controlled.

Figure 7 presents the excitation spectra, for the 614 nm emission peak, for the unfired samples as a function of europium concentration. The spectra are again normalized around the 397 nm excitation peak. The excitation spectra manifest five main peaks: 397, 416, 466, 536, and 588 nm. As the europium content is increased, the relative intensities of the excitation peaks change. With the spectra normalized around the 397 nm peak, the 466 and 588 nm peaks remain relatively unchanged, while the intensity of the peaks at 416 and 536 nm become stronger with increasing europium content. This suggests that there are two distinct europium environments present in the amorphous material, and that one is preferentially occupied at low europium concentrations (i.e., the site which is excited by 397, 466, and 588 nm radiation). Consideration of the emission band at 592 nm, which grows together with the 702 nm line also suggests that the source of the emission is a europium ion in a different environment in the titania lattice. This comes from the observation that europium-containing phosphors whose main

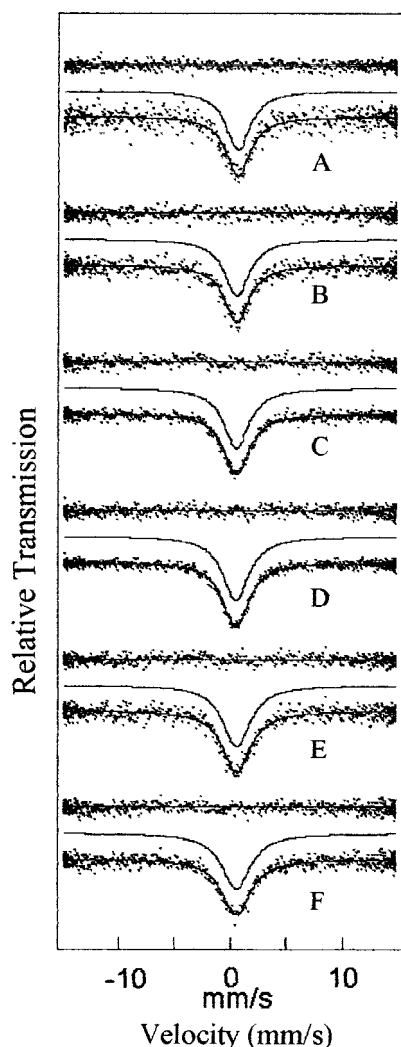


**Figure 5.** Mössbauer spectra for the unfired samples doped with different levels of europium. (A)  $x = 0.00794$ , (B)  $x = 0.00476$ , (C)  $x = 0.00318$ , (D)  $x = 0.00159$ , (E)  $x = 0.000794$ , and (F)  $x = 0.000397$ .

**TABLE 1:  $^{151}\text{Eu}$  Mössbauer Data from Unfired Samples Doped with Varying Levels of Europium Showing Trends in Isomer Shifts and Linewidths**

Eu concentration (%)	peak width (mm/s)	isomer shift (mm/s)
0.000397	2.61	0.58
0.000794	2.70	0.50
0.00159	2.77	0.48
0.00318	2.83	0.49
0.00476	3.01	0.55
0.00794	3.11	0.52

emission band is in the range 610 nm to 630 nm tend to have no inversion symmetry, while those whose main emission band is in the region up to 600 nm tend to have a site of inversion symmetry.<sup>2</sup> This then agrees well with the data from both the Raman study, and the Mössbauer analysis.

Titania itself has an optical band gap of 386 nm for anatase, and 412 nm for rutile. There have been no reports to our knowledge for the band gap in the amorphous system. Titania samples prepared in the absence of europium gave no emission spectrum. The sample prepared in the absence of titania (i.e., the europium precipitate) exhibited a very similar excitation spectrum to the europium titania samples, but with an extra band at shorter wavelength (320 nm). If excitation were via the excitation of electrons across the titania band gap from the val-

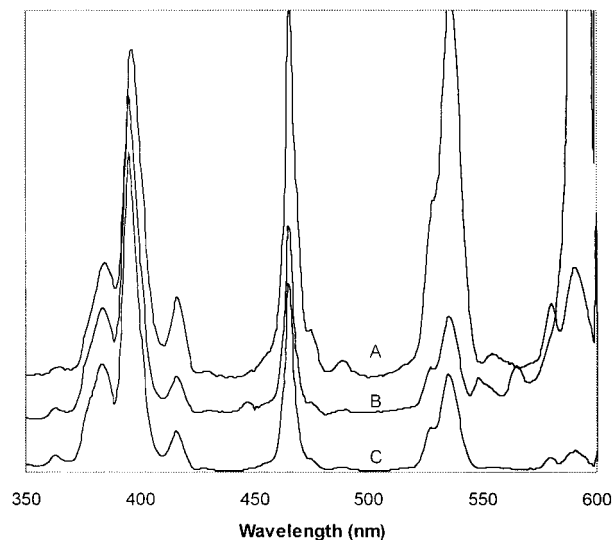


**Figure 6.** Excitation spectra for unfired titania doped with a europium content of  $x = 0.00794$ . Excitations are for emissions at A = 614 nm, B = 592 nm, C = 702 nm.

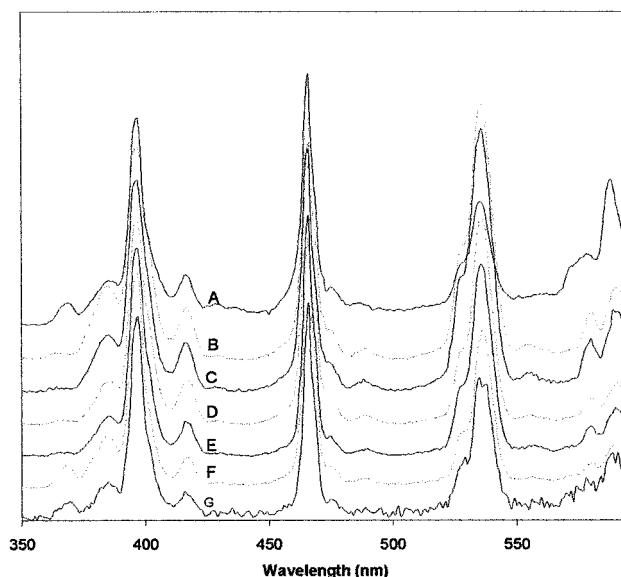


**Figure 7.** Excitation spectra for the 614 nm emission from unfired samples with different europium concentrations. (A) hydrothermal ( $x=0.00318$ ), (B)  $x = 0.00794$ , (C)  $x = 0.00476$ , (D)  $x = 0.00318$ , (E)  $x = 0.00159$ , (F)  $x = 0.000794$ , (G)  $x = 0.000397$ .

ence to conduction bands, followed by a nonradiative relaxation into the europium  $^5\text{D}$  levels, then the excitation spectrum should show some evidence of an absorption edge, which is not in fact observed. Therefore, we can say that the luminance in the amorphous sample is purely due to the direct excitation of the  $\text{Eu}^{3+}$  ions, and not the excitation of defects in the amorphous host.

**Effect of Calcining the Amorphous Material.** In addition to studying the effect of europium concentration on the brightness of the phosphors, the effect of calcination of the phosphors was also investigated. It was found that increasing the europium content increased the temperature, almost linearly, for the crystallization of the amorphous material to anatase (Figure 8). The simple relationship between the europium content and the crystallization temperature also allows facile determination of the europium content using DSC. This is a surprising result, since the doping of a 3+ metal ion into the titania to replace the 4+ titanium ion would be expected to result in an increase



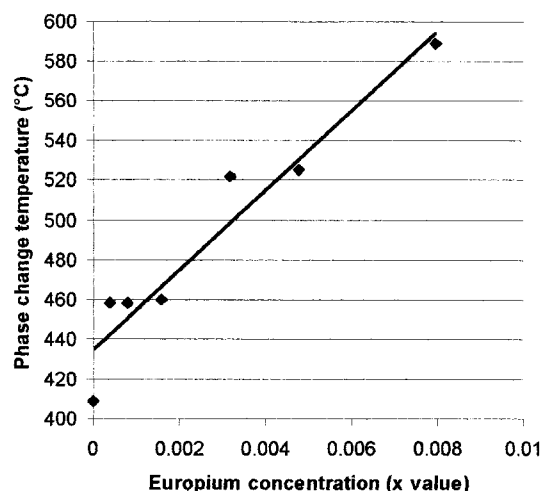


**Figure 8.** Graph of crystallization temperature vs europium doping level for amorphous materials fired in air for 1 h.

in the number of oxygen ion vacancies. Such an increase would be expected to facilitate easier solid state rearrangement of the ions, and so lower the temperature required for crystallization.<sup>14–18</sup> Since, however, the crystallization temperature is raised, this observation points to the incorporation of the europium into the lattice in positions other than on the titanium lattice sites, therefore reducing the number of oxygen ion vacancies.

Analysis of the structures of anatase, brookite, and rutile also shows that although there are holes present in all three structures, the holes in rutile are not large enough to accommodate the large  $\text{Eu}^{3+}$  ion without some expansion of the lattice. The anatase and brookite holes, however, are larger, and therefore shifts in unit cell dimensions would be harder to detect. There are no significant changes in the positions of the anatase XRD peaks after calcination at 600 °C with increasing europium content. They are, however, broader than their undoped analogues indicating either that the crystallization process has been hindered by the europium, or that there is a range of slightly different cell sizes in the different particles. A shift to lower  $2\theta$  would be expected if a significant proportion of the titanium ions (ionic radius = 0.68 Å) were replaced by the much larger europium ions (ionic radius = 0.95 Å),<sup>19</sup> since the planes of ions would be forced further apart. Calcination at 1000 °C forms rutile; however, in this case a shift to low angle in the positions of the rutile peaks can be observed. This is in keeping with some of the europium entering the lattice, forcing the atomic planes further apart (due to the larger size of the  $\text{Eu}^{3+}$  compared to  $\text{Ti}^{4+}$ ). In the rutile lattice, the distorted octahedral holes present are significantly larger than the titanium ion sites themselves, indicating that the europium ions would sit in these holes, as they require only slight distortion to seat  $\text{Eu}^{3+}$  ions comfortably. The rutile unit cell dimensions for the material with a europium concentration of  $x = 0.00794$  (calcined at 1000 °C for 1 h) were  $a = 4.600$  Å, and  $b = 2.959$  Å, whereas the undoped rutile, measured on the same XRD powder diffractometer, had dimensions  $a = 4.539$  Å and  $c = 2.950$  Å (significantly smaller). Furthermore, at high europium concentration ( $x = 0.00794$ ), a second phase (identified as  $\beta\text{-Eu}_2\text{Ti}_2\text{O}_7$  by XRD) was observed in addition to the rutile phase.

In addition to the changes in crystallization temperature, it was also noted, that increasing the firing temperature decreased the brightness of the phosphors (Figure 9). XRD was used to monitor the phase changes in the material with europium concentration at  $x = 0.00318$  (Figure 10). This was possible due to the shift to higher  $2\theta$  of the anatase 101 peak ( $2\theta =$

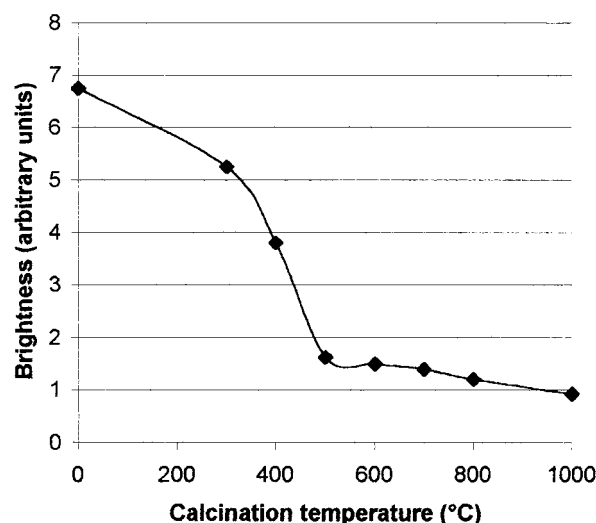


**Figure 9.** Graph of brightness vs calcination temperatures for sample doped with a europium of  $x = 0.00318$ , calcined for 1 h.

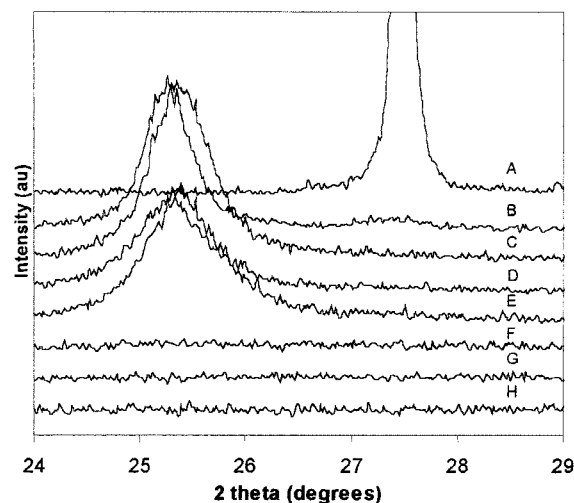


**Figure 10.** XRD spectra showing the progressive phase change from amorphous powder to rutile for samples with a europium content of  $x = 0.00318$ . (A) 1000 °C, (B) 800 °C, (C) 700 °C, (D) 600 °C, (E) 500 °C, (F) 400 °C, (G) 300 °C, (H) unfired.

25.28°) due to overlap with the brookite 120, and 111 peaks ( $2\theta = 25.34^\circ$ , and  $25.69^\circ$ , respectively).<sup>15</sup> Below 500 °C, no crystallization was observed, but at midrange temperatures (500 °C–700 °C) brookite was present as a secondary phase to the main product, anatase. At 800 °C, anatase and no brookite was present, but some rutile had formed. At 1000 °C only rutile was present. This shows that as the amorphous phase crystallizes, the brightness of the phosphor decreases.

Figure 11 shows the  $\text{Eu}^{151}$  Mössbauer spectra for the titania samples with europium concentration at  $x = 0.00318$ , calcined at different temperatures. There is a clear increase in line width as the calcination temperature is increased toward 500 °C, indicating the development of multiple lattice sites for the europium within the titania lattices. This agrees well with the XRD, which shows the presence of brookite in addition to anatase. In addition, the isomer shift increased with calcination temperature up to 500 °C, indicating that the europium environments are changing to become more covalent in their bonding. Above 500 °C, both the width and the isomer shifts decrease with increasing temperature, as does the relative amount of anatase to brookite (XRD). These results suggest that the europium occupies sites in both the anatase (tetrag-

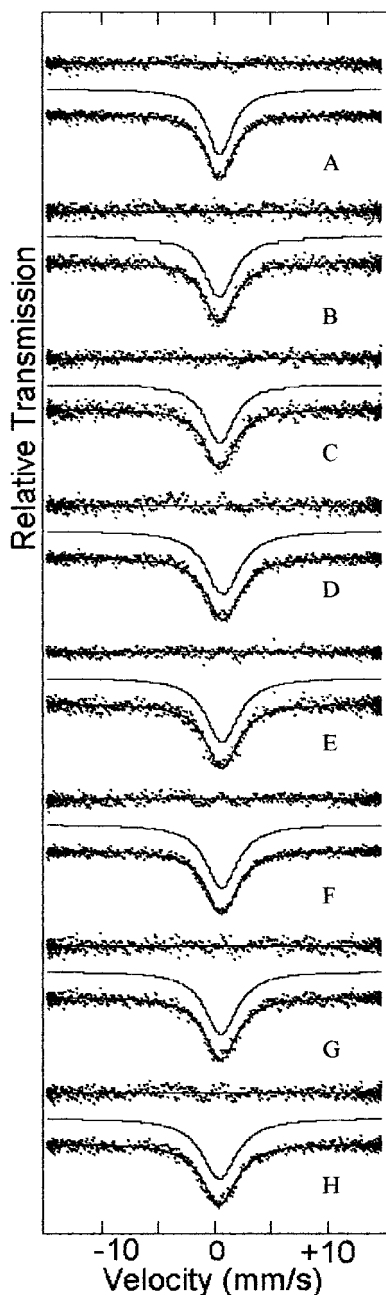


**Figure 11.** Mössbauer spectra for samples doped with europium content of  $x = 0.00318$ , and calcined at various temperatures for 1 h. (A) unfired, (B) 300 °C, (C) 400 °C, (D) 500 °C, (E) 600 °C, (F) 700 °C, (G) 800 °C, (H) 1000 °C.

onal) and brookite (orthorhombic) lattices. The rutile (tetragonal) sample (fired at 1000 °C) again exhibits a smaller isomer shift and greater width, indicating multiple sites with greater ionic character in the bonding than the earlier phases. Table 2 shows the widths and isomer shifts for the Mössbauer spectra.

Excitation spectra were also measured for the calcined samples of the titania with europium at a concentration of  $x = 0.00318$  (Figure 12). Again the excitation spectra for the 614 nm emission were measured. This time the spectra were normalized around the 466 nm peak. The peak at 397 nm changed significantly as the calcination temperature was increased up to 800 °C, on average decreasing with the increasing temperature, particularly up to the anatase crystallization temperature (500 °C). The small side peak at 416 nm, however, remained relatively unchanged. When the powder was fully

**TABLE 2:**  $^{151}\text{Eu}$  Mössbauer Data from Fired Samples Doped with Europium Content  $x = 0.00318$ , Showing Trends in Isomer Shifts and Linewidths

calcination temperature (°C)	peak width (mm/s)	isomer shift (mm/s)
unfired	2.86	0.47
300	3.17	0.43
400	3.13	0.46
500	3.63	0.74
600	3.52	0.65
700	3.41	0.60
800	3.48	0.53
1000	3.73	0.38
hydrothermal	2.85	0.49

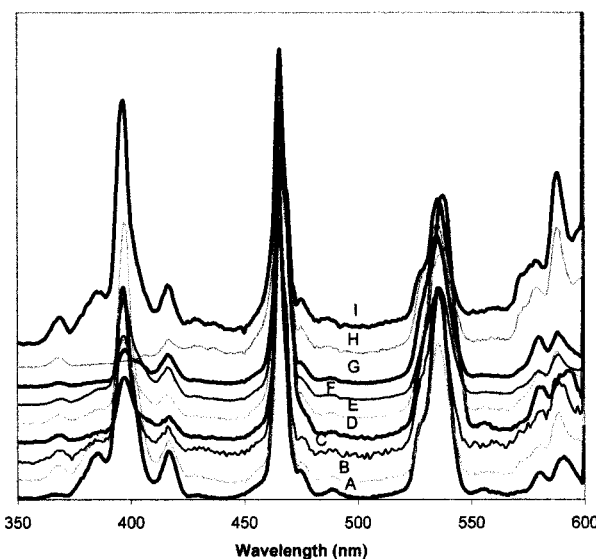


**Figure 12.** Excitation spectra for samples doped with a europium content of  $x = 0.00318$ , and calcined at various temperatures for 1 h. (A) unfired, (B) 300 °C, (C) 400 °C, (D) 500 °C, (E) 600 °C, (F) 700 °C, (G) 800 °C, (H) 1000 °C, (I) hydrothermal.

transformed to rutile at 1000 °C, the peak at 397 nm almost completely disappeared. The peak at 536 nm remained relatively unchanged throughout the calcination and phase transformation process. The peak at 588 nm also remained relatively unchanged as the calcination temperature was increased, except for the final temperature (1000 °C) which showed a slightly stronger excitation. These results can be explained in terms of the reduction in size of the optical band gap of the titania as it is calcined. The band gap in the amorphous material will be poorly defined due to its lack of ordered crystal structure, and will be larger than for the crystalline titania polymorphs. As the samples crystallize, the band gap is reduced, and the tail of the conduction band begins to overlap with the highest energy, initial excited-state energy levels in the europium ions. This results in some quenching of the 397 nm excitation as electrons promoted to this excited state can escape to the conduction band, and so do not result in luminescence. The other excitations at longer wavelength are not affected since the excited-state energies are well below the conduction band of the titania. When the titania is transformed to rutile at high temperature, the band gap moves to much lower energy (from 386 to 412 nm). This puts the europium excited state energy level which is populated by the 397 nm excitation, squarely in the conduction band of the titania (rutile), and so this excitation is effectively quenched.

Since a phase mixture persisted throughout the firing range up to 800 °C, hydrothermal processing was used to prepare a sample of pure anatase phase. Hydrothermal processing has been shown to be capable of producing highly crystalline phase pure

anatase.<sup>20</sup> The Mössbauer spectrum of this  $\text{Eu}^{3+}$ -doped material was much narrower than the anatase prepared by calcination (Table 2), indicating that the europium occupied only one site in anatase itself. The excitation spectrum was also measured for the 614 nm emission (Figure 12). Interestingly, the relative intensities of the peaks in the spectrum were somewhat different from those for the powders calcined between 500 and 800 °C. From XRD it is clear that brookite only forms a small part of the phase mixture, yet from the excitation spectra, it is equally clear that this small amount of brookite must be the source of most of the light emission from the calcined titania.

The apparently erratic increases and decreases in the relative intensity of the excitation peak at 397 nm for the calcined samples (Figure 12), can also give us some insight into the formation of the anatase and brookite, since unlike other analysis techniques, these spectra are particularly sensitive to the presence of small amounts of brookite. From Figure 12, we can see that after calcination at 300 °C the excitation spectrum begins to approach that of anatase, with a strong 397 nm excitation. After calcination at 400 °C, however, this peak becomes relatively weaker, and the spectrum begins to more resemble brookite. This continues up to 500 °C (at which point both anatase and a little brookite are detectable by XRD). This suggests that during calcination, anatase forms initially, and it is only at higher temperatures (above 300 °C) that the brookite is formed. Above 500 °C, the excitation spectrum begins to return toward that of anatase, and indeed XRD shows that the ratio of anatase to brookite increases. At 800 °C, however, there is a sudden change, and the excitation spectra are again reversed as rutile begins to form. At 1000 °C the anatase has been completely converted to rutile, and the peak at 397 nm disappears. This type of analysis could prove very useful in studying the phase transformations in titania, which can otherwise be very difficult to follow. It may also be possible to adapt the technique to other ceramic systems where phase changes occur, by doping a small amount of rare earth activator to develop an emission site. Furthermore, it also gives us some indication that the band gap for brookite (which to our knowledge is currently unreported) lies in the region below anatase, (lower energy than 386 nm) since the 397 nm emission is partly quenched when brookite and anatase are in a mixture together.

These results demonstrate that there is one potential site for europium in anatase with a primary excitation at 397 nm. The primary excitation for brookite is 536 nm, but it is not clear how many sites are present in brookite since it could not be prepared in a phase pure form. The Raman spectrometer was used to examine more closely the Stokes emission band at 702 nm in the calcined samples. Figure 13 shows the development of two different bands (702 and 715 nm) in the temperature range 500 °C to 800 °C for the sample containing a europium concentration of  $x = 0.00318$ . Since the pure anatase sample does not emit in this region, and the ratios of the intensities of these bands change with temperature, it seems that there are two sites for europium in the brookite lattice.

A similar shift in intensities was observed for samples containing europium concentrations at both  $x = 0.000397$  content and  $x = 0.00794$  (Figure 14). The shift toward increased relative intensity in the 702 nm band (and 592 nm band) occurred at lower calcination temperature in the  $x = 0.00794$  europium sample. Since the crystallization temperature of anatase in this sample is higher, this is further evidence that both bands are due to brookite. The rutile structure possesses only one potential europium site (though the Mössbauer spectrum is broad, suggesting a number of different cell sizes)

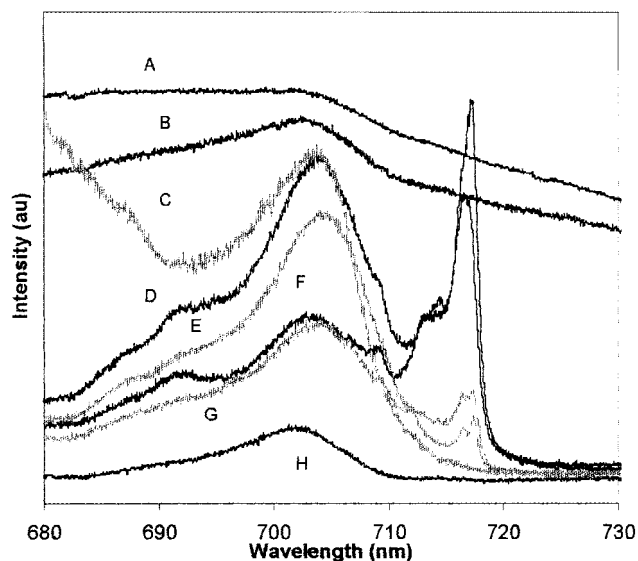


**Figure 13.** Down conversion luminescent spectra obtained using a Raman spectrometer for samples doped with a europium content of  $x = 0.00318$ , and calcined for 1 h at different temperatures. (A) 400 °C, (B) 300 °C, (C) 1000 °C, (D) 600 °C, (E) 800 °C, (F) 500 °C, (G) 700 °C, (H) unfired.

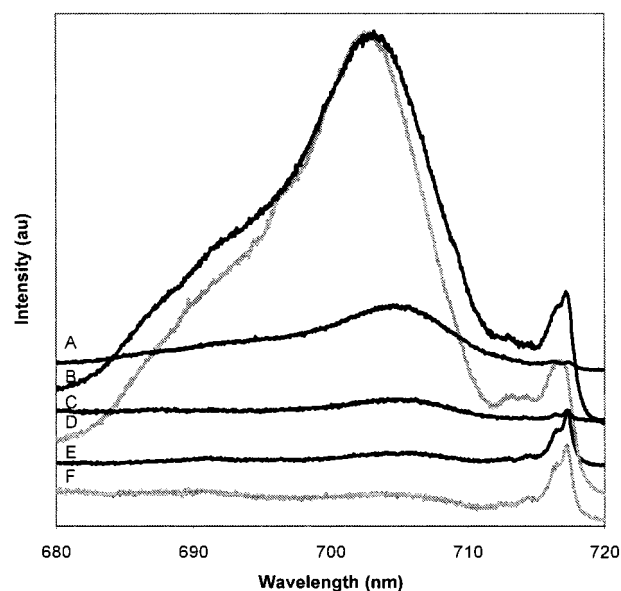


**Figure 14.** Down conversion luminescent spectra obtained using a Raman spectrometer for samples with europium concentrations of  $x = 0.000397$  or  $x = 0.00794$ , and calcined at different temperatures. (A)  $x = 0.00794$ , 800 °C, (B)  $x = 0.00794$ , 600 °C, (C)  $x = 0.00794$ , 500 °C, (D)  $x = 0.000397$ , 800 °C, (E)  $x = 0.000397$ , 600 °C, (F)  $x = 0.000397$ , 500 °C.

which causes limited luminescence. The second europium environment results from the formation of the  $\beta\text{-Eu}_2\text{Ti}_2\text{O}_7$  phase. The amorphous material also contains at least two europium environments, which both luminesce. The excitation spectrum of the amorphous material resembles that for the anatase material more than the brookite material, but as europium concentration increases, so does its resemblance to the brookite material.

## Conclusions

A number of europium-doped titania phosphors have been prepared and their luminescent properties measured. The maximum luminescent brightness in any of these phosphors is that of the amorphous material doped with europium at a

concentration of  $x = 0.00794$ . This amorphous titania contains at least two sites for the europium in its matrix, while in the anatase phase, there is only one. Brookite has also been shown to have at least two potential luminescent sites for europium. The rutile phase again has only one site, although its cell size may vary from grain to grain depending on the  $\text{Eu}^{3+}$  content. We have shown via a distinct difference in the cell size, that the rutile lattice is capable of accommodating the europium ions in the holes present in the lattice. At high  $\text{Eu}^{3+}$  contents, the second (non-luminescent) site may well be the result of the formation of the second phase  $\beta\text{-Eu}_2\text{Ti}_2\text{O}_7$ . This phase caused broadening in the Mössbauer spectra at 1000 °C as its Mössbauer parameters are different to those of the  $\text{TiO}_2$  phase.

Increasing the amount of europium in the material has been shown to increase the crystallization temperature, and this is evidence that the europium does not lie on the titanium ion sites in the lattice, but is present in the holes. This would mean that the given formulation of  $\text{Ti}_{1-3x}\text{Eu}_{4x}\text{O}_2$  is incorrect and it is better written  $\text{TiEu}_x\text{O}_{2+3x/2}$ . Further analysis of the excitation spectra has also suggested that the brookite phase begins to form after the anatase has begun to crystallize during calcination, and that the brookite phase will be a more suitable lattice for the production of bright phosphors, particularly if excited at longer wavelengths. The measurement of excitation spectra has been shown to be a useful tool in investigating not only the luminescent properties of titania, but also its crystallization characteristics. This technique may find further application in other systems.

**Acknowledgment.** J.S. thanks the TCS for support of J.O. The authors also thank the referees for their useful comments.

J.S. and R.W. acknowledge the support of the ESPRC (GR/L41370) for the funding of the Labram Raman spectrometer.

## References and Notes

- (1) Ozawa, L. *Cathodoluminescence Theory and Applications*; VCH Publishers: New York, 1990; Chapter 4.
- (2) Kano, T. *Phosphor Handbook*; CRC: Boca Raton, FL, 1998; Chapter 3.
- (3) Unpublished preliminary results.
- (4) Iida, Y.; Furukawa, M.; Kato, K.; Morikawa, H. *Appl. Spectrosc.* **1997**, *51* (5), 673.
- (5) Schlotter, P.; Baur, J.; Hielscher, C.; Kunzer, M.; Obloh, H.; Schmidt, R.; Schneider, J. *Mater. Sci. Eng. B—Solid* **1999**, *59* 6(1–3), 390.
- (6) Ovenstone, J.; Yanagisawa, K. *High-Pressure Research*, in press.
- (7) Hattori, A.; Yamamoto, M.; Tada, H.; Ito, S. *Chem. Lett.* **1998**, *8*, 707.
- (8) Ohtani, B.; Bowman, R. M.; Colombo, D. B., Jr.; Kominami, H.; Noguchi, H.; Uosaki, K. *Chem. Lett.* **1998**, *14*, 579.
- (9) Ichinose, H.; Kawahara, A.; Katsuki, H. *J. Ceram. Soc. Jpn.* **1996**, *104*, 914.
- (10) Kominami, H.; Matsuura, T.; Iwai, K.; Ohtani, B.; Nishimoto, S.; Kera, Y. *Chem. Lett.* **1995**, *11*, 693.
- (11) Fox, M. A.; Dulay, M. T. *Chem. Rev.* **1993**, *93*, 341.
- (12) Sclafani, A.; Palmisano, L.; Schiavello, M. *J. Phys. Chem. B* **1990**, *94*, 829.
- (13) Hider, R. C.; Howlin, B.; Miller, J. R.; Rahim, A.; Mohd-Nor; Silver, J. *Inorg. Chim. Acta* **1983**, *80*, 51–56.
- (14) Amersham product information.
- (15) Ohtsuka, Y.; Fujiki, Y.; Suzuki, Y. *J. Jpn. Assoc. Min.* **1982**, *77*, 117.
- (16) Heald, E. F.; Weiss, C. W. *Am. Mineral.* **1972**, *57*, 10.
- (17) Genari, F. C.; Pasquevich, D. M. *J. Mater. Sci.* **1998**, *33*, 1571.
- (18) Hishita, S.; Takata, M.; Yanagida, H. *Yogyo-Kyokai-shi* **1978**, *86* (12), 631.
- (19) Ovenstone, J.; Yanagisawa, K. *Chem. Mater.* **1999**, *11* (10), 2770.
- (20) Shannon, R. D. *Acta Crystallogr.* **1976**, *A32*, 151.
- (21) Yanagisawa, K.; Ovenstone, J. *J. Phys. Chem. B* **1999**, *10* (37), 7781.